Transactions, SMiRT-22
San Francisco, California, USA - August 18-23, 2013
Division IX (include assigned division number from I to X)

CHARACTERISTICS OF SIMULATED GROUND MOTIONS CONSISTENT WITH SEISMIC HAZARD

Akemi Nishida[1], Sayaka Igarashi[2], Shigehiro Sakamoto[2], Yasuo Uchiyama[2], Yu Yamamoto[2], Ken Muramatsu[3], and Tsuyoshi Takada[4]

[1] Center for Computational Science and e-Systems, Japan Atomic Energy Agency, Kashiwa, Japan (nishida.akemi@jaea.go.jp)
[2] Technology Center, Taisei Corporation, Yokohama, Japan
[3] Professor, Department of Nuclear Safety Engineering, Tokyo City University, Tokyo, Japan
[4] Professor, Department of Architecture, The University of Tokyo, Tokyo, Japan

ABSTRACT

Most probabilistic risk assessments (PRA) of structures involve the use of probabilistic schemes such as the scheme using probabilistic seismic hazard and fragility curves. Even when earthquake ground motions are required in Monte Carlo Simulations (MCS), they are generated to fit the specified response spectra, such as uniform hazard spectra at a specified exceedance probability. These ground motions, however, are not directly linked with corresponding seismic source characteristics.

In this context, the authors propose a methodology based on MCS to reproduce a set of input ground motions to develop an advanced PRA scheme that can explain the exceedance probability and sequence of functional loss in a nuclear power plant. These generated motions are consistent with the seismic hazard for the target site and their seismic source characteristics can be recognized in detail.

Ground motions reproduction is conducted for the target site, Oarai (Japan), location of the subject nuclear power plant. 200 ground motions ranging from 700 to 1,100 cm/s^2 of maximum acceleration are reproduced. Seismic sources for reproducing these motions are selected according to their contributions to the hazard of the site, and the ground motion generations with stochastic parameters for the seismic source characteristics are conducted repeatedly until the ground motions with the target maximum acceleration are obtained.

Consequently, about 100,000 generations were required for reproducing 200 motions. Acceleration deviations of reproduced motions for 1,000 to 1,100 cm/s^2 distribute from 1.5 to 3.0, for example, and deviations of 1.0 to 3.0 for stress drops are required for obtaining these acceleration deviations. It is also shown that reproduced ground motions incorporate the differences between each seismic source characteristics and they are effectively available for PRA of structures.

INTRODUCTION

Seismic safety evaluation of nuclear power plants has been regarded a significant subject in recent years. Research and development of various methodologies for probabilistic risk assessment (PRA) have been conducted. In general, probabilistic schemes such as probabilistic seismic hazard and fragility curves without time histories of earthquake ground motions are employed in performing PRAs of structures,. Even in cases where earthquake ground motions are used in Monte Carlo Simulations (MCS), ground motions are generated so that they fit to the specified response spectra, e.g., uniform hazard spectra at a specified exceedance probability. It is, however, one of problems that these ground motions are not directly linked with seismic source characteristics. Here, the authors propose a methodology to reproduce a set of ground motions that is consistent with the seismic hazard of the target site and is considering the differences between seismic source characteristics in order to develop an advanced PRA scheme based on MCS.

In this paper, firstly, an outline of PRA and the concept of hazard-consistent ground motions reproduction are presented. Secondly, characteristics of ground motions that are obtained by the proposed method and the relationship between seismic source characteristic and maximum accelerations of these motions are shown.

OUTLINE OF PROBABILISTIC RISK ASSESSMENT

At present, various methodologies are utilized to perform PRAs for structures. Table 1 summarizes the methods available for seismic hazard analysis.

Table 1: Methods of seismic hazard analysis for PRA.

Methods of seismic hazard analysis for PRA	Comments
(1) Probabilistic seismic hazard curves 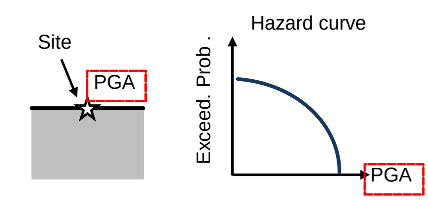 	・A simple commonly-used method for PRA. ・Seismic hazard is evaluated based on a ground-motion intensity index such as PGA; therefore, frequency content and duration characteristics cannot be considered. ・Differences of seismic sources and their microscopic characteristics cannot be considered.
(2) Fitting simulated ground motions to uniform hazard spectra (UHS) 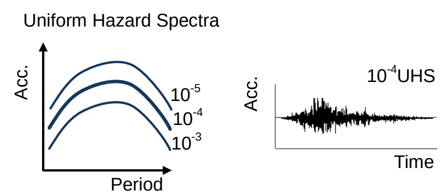 	・Ground motions are generated so that they fit UHS. ・Frequency content and duration characteristics can be considered. ・Generated ground motions show averaged characteristics for all sources, so differences of seismic sources and their microscopic characteristics cannot be considered.
(3) Fitting simulated ground motions to response spectra of an M-R attenuation relationship 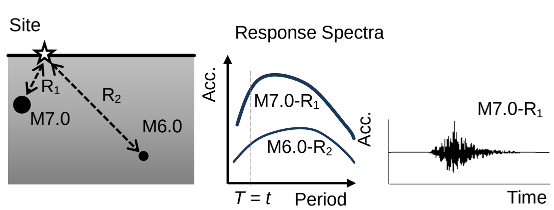 	・Seismic sources that cause strong ground motions on the site are selected. Earthquake occurrence rates for seismic sources are specified. ・Ground motions are fitted to the response spectra of an M-R attenuation relationship, which shows the averaged characteristics of ground motions from the selected M-R source. ・Differences of seismic sources can be considered, while variations of their microscopic source characteristics cannot be considered. ・The relationship between generated ground motions and the hazard curve is not clear.
(4) Fault model and rupture model 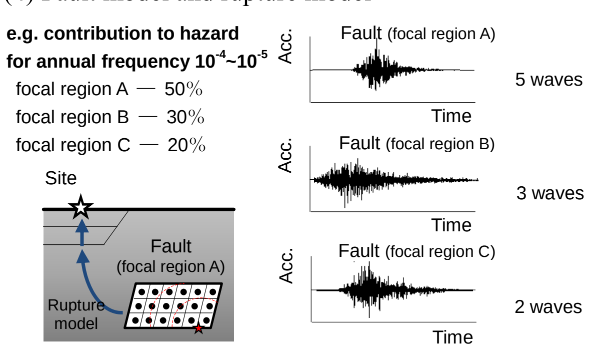 	・Seismic sources are decided based on their contribution to the hazard of the site. ・Ground motions are generated from fault models and fault rupture models so that they are consistent with site-specific hazards. ・Differences of seismic sources and variations of their microscopic characteristics can be considered. ・Propagation characteristics can be considered. ・The relationship between a seismic source which caused damage and the damage are easy to understand.

Method (1), where a probabilistic seismic hazard curve is obtained, is the most general and simplest approach used in PRA. In this method, seismic hazard is evaluated based on the ground-motion intensity index such as peak ground acceleration (PGA) without generating ground motions. Frequency content and duration characteristics are not incorporated in the evaluation. Inevitably, much information about external forces, which are related to damages of structures and/or equipment, is lost and cut off at “Pinch point” quoted by Sewell et al (2009).

Method (2), where ground motions are generated so that they fit the uniform hazard spectra (UHS) at a specified exceedance probability, can well take account of frequency content and duration characteristics, compared with Method (1). In addition, generated ground motions are related with the exceedance probability in whole frequencies. However, the characteristics of generated motions are averaged because differences of seismic sources are not considered.

In Method (3), seismic sources that create intense ground motions at the site are selected. And, for each selected seismic source, which is defined by magnitude (*M*) and distance (*R*), ground motions are generated so that they fit the response spectra via an *M-R* attenuation relationship. Here, the attenuation relationship is the averaged characteristics of ground motions from the specified *M-R* sources, so the generated ground motions do not incorporate the variations in microscopic characteristics of the sources. Moreover, earthquake occurrence rates for selected sources may be specified, but the relationship between generated ground motions and the hazard curve is not clear.

Method (4) corresponds with the method proposed in this paper. Fault models and fault rupture models are employed for generating ground motions, where the variations of sources microscopic characteristics are defined such that the distribution of ground motion intensity matches that of the attenuation relationship. These generated motions are consistent with the seismic hazard, considering the differences of seismic sources, the variations of source characteristics, and propagation characteristics. As mentioned above, the authors propose a methodology based on MCS to generate a set of ground motions consistent with the seismic hazard and to consider differences in source characteristic.

SEISMIC HAZARD ANALYSIS

Ground motions reproduction is conducted for the target site, Oarai, Japan (Lat. 36.26ºN, Lon. 140.55ºE), where the subject nuclear power plant is located. Figure 1 shows the seismic hazard curve at the site. The seismic hazard is evaluated based on the method of HERP (2009), where the index of the ground motion intensity is the maximum acceleration on the free rock surface. The attenuation relationship proposed by Si and Midorikawa (1999) is adapted with the variation of 0.25 (common-logarithm standard deviation). The attenuation relationship by Si and Midorikawa is shown in Eq.(1). Here, in seismic hazard analysis, the acceleration calculated from Eq.(1) is divided by the constant 1.4, because the PGA in Eq.(1) is the maximum acceleration on the ground surface.

$$\log \mathrm{PGA} = 0.5M_w + 0.0043H + d + 0.61 - \log(R + 0.0055 \times 10^{0.5M_w}) - 0.003R \tag{1}$$

where M_w is moment magnitude, d is fault type constant, H is focal depth (km), and R is fault distance (km).

In this study, the target of the ground motions reproduction is the annual exceedance probability of 10^{-5}, which is the safety target for the reactor containment vessel, and which corresponds to maximum acceleration of 1,100 cm/s^2. In addition, in order to assess the safety of the structure for ground motions that exceed the design motions, it is decided that ground motions from 700 to 1,100 cm/s^2 should be reproduced. Therefore, the acceleration range from 700 to 1,100 cm/s^2 was divided into 4 intervals of 100 cm/s^2 each, and then, 50 ground motions were reproduced for each range, i.e., a total of 200 ground motions were reproduced. Seismic sources that are used for the ground motions reproduction are selected according to their contributions to the hazard, and the number of reproduced ground motions was decided for each sources. Table 2 shows the contribution ratio and the decided number of ground motions for each seismic source. In addition, the number of reproduced motions from each seismic source was classified by the magnitude and the distance according to their contribution to the hazard. Figure 2 shows an example of the number of ground motions classified in the group of Fault-specified earthquakes in the Southern Kanto, inter-plate earthquakes of Philippine Sea plate (upper 1,000 cm/s^2).

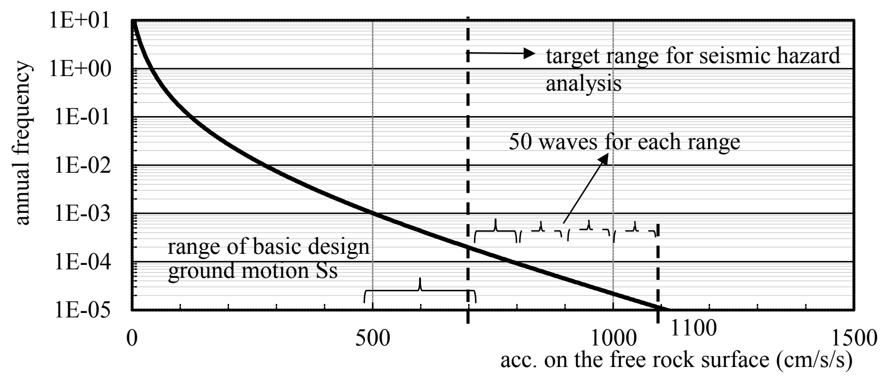

Figure 1. Seismic hazard at the site, Oarai.

Table 2 : Contribution ratio and the number of ground motions.

Source	700 ~ 800 (cm/s^2)		800 ~ 900 (cm/s^2)		900 ~ 1000 (cm/s^2)		1000 ~ (cm/s^2)	
	C (%)	*N*	*C* (%)	*N*	*C* (%)	*N*	*C* (%)	*N*
(1) Fault-specified earthquakes in the Southern Kanto	45.4	23	50.5	25	56.2	28	67.1	33
(2) Tsunami earthquakes from Sanriku-Oki to Boso-Oki along Japan Trench (earthquakes along Japan Trench)	3.6	2	4.0	2	4.4	2	3.9	2
(3) Fault-unspecified earthquakes in the Southern Kanto	15.8	8	12.0	6	8.4	4	3.1	2
(4) Fault-unspecified pacific plate earthquakes	30.2	15	27.1	14	23.1	12	13.4	7
(5) Fault-unspecified Crustal earthquakes	5.1	2	6.4	3	7.9	4	12.5	6
Total	100.0	50	100.0	50	100.0	50	100.0	50

where, *C*: Contribution to the hazard, *N*: The number of ground motions to be reproduced

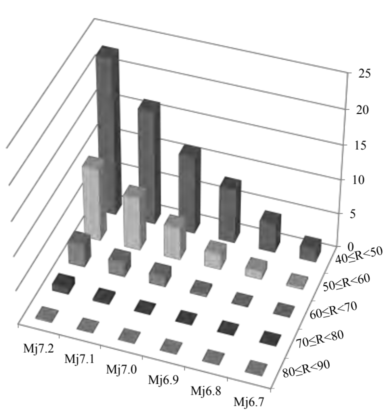

(1) Fault-specified earthquakes in the Southern Kanto

(Interplate earthquake of Philippine Sea plate 1,000cm/s^2 upper)

	JMA Magnitude Mj					
Fault distance	6.7	6.8	6.9	7.0	7.1	7.2
R = 40 ~ 50km	1	1	3	4	5	7
R = 50 ~ 60km	0	0	1	2	3	4
R = 60 ~ 70km	0	0	0	0	1	1
R = 70 ~ 80km	0	0	0	0	0	0
R = 80km ~	0	0	0	0	0	0
					Total (waves)	33

Figure 2. Contribution classified by magnitude and distance / the number of ground motions.

REPRODUCTION METHOD OF GROUND MOTIONS CONSISTENT WITH HAZARD

The ground motions used in this study were generated by the stochastic Green's function method (Boore et al. (1983), Kamae et al. (1991), Irikura et al. (1997), Satoh et al (1994b)), where the seismic source characteristics have stochastic parameters so that the PGA of generated ground motions fit the seismic hazard by the attenuation relationship with 0.25 of variation. In the simulation for ground motion generations, only aleatory uncertainty for microscopic seismic source characteristics are considered, while other uncertainty such as macroscopic seismic source characteristics and epistemic uncertainty about microscopic seismic source characteristics are not considered, in order to control the number of MCS.

The median of the maximum acceleration of ground motions generated by the stochastic Green's function method does not completely correspond to that of the attenuation relationship as it is, particularly for ground motions of having a distant source. Therefore, the constant coefficient is multiplied to the acceleration of the generated ground motions to fit the median acceleration of the attenuation relationship.

Table 3 shows stochastic parameters in seismic source characteristics for the stochastic Green's function base on Eqs. (2) through (7). The variations for these parameters are set based on previous studies, and are adjusted based on a sensitivity analysis of each seismic source characteristics so that the variations of maximum acceleration of generated motions are consistent with those of the attenuation relationship.

For reproducing ground motions, several faults containing stochastic parameters of seismic sources characteristics are set in each group of seismic sources that are divided by region, magnitude, and distance. In MCS, the ground motions are repeatedly generated one by one for each fault where realization values for stochastic parameters are given in the way that realization values are randomly set according to the corresponding distribution of stochastic parameter. When the maximum acceleration of the generated motion is included in the acceleration range from 700 to 1,100 cm/s^2, the motion is extracted as the reproduced motion. The ground motion that is satisfied with target maximum acceleration is extracted according to the generation order. Ground motion generations are continued until a total of 200 motions are extracted.

Table 3: Stochastic parameters for seismic source characteristics.

stochastic parameters for seismic source characteristics	name	unit	distribution	λ or μ	ζ or σ			reference
					Others	Japan Trench	Crustal	
stress drop	$\Delta\sigma$	MPa	lognormal	3.0, 5.0, 14.0	0.60	0.42	0.48	Satoh(2004) Dan et al.(2001) Kawase et al.(2004) Tsurugi et al.(2006)
shear wave ratio to rupture velocity	C_{Vr}	---		0.72	0.10	0.07	0.08	Geller(1976)
rise time of coefficient	α_{tr}	---		0.5	0.20	0.14	0.16	HERP (2009)
rupture starting points	startX	---	uniform	on the bottom of the asperity				Itoi et al.(2009) Mai et al.(2005)
location of the asperity	aspX, aspY	---		in the fault plane				
asperity area ratio	C_{Sa}	---	normal	0.22	0.04	0.04	0.04	Masuda et al.(2006)
frequency for high-cut filter	f_{max}	Hz	lognormal	6.0, 13.5, 13.5	0.60	0.42	0.48	Satoh et al.(1994a) Satoh et al.(2000)
Q-value coefficient	C_{Qc}	---		110.0	0.20	0.14	0.16	AIJ(2004)
	C_{Qp}	---		0.69	0.20	0.14	0.16	

where, λ : median, μ : average, ζ : log-standard deviation, σ : standard deviation
λ (μ) of $\Delta\sigma$ or f_{max} represent the value for crustal earthquakes, inter-plate earthquakes, intra-plate earthquakes from the top.

$$A(f) = \frac{R_{\theta\phi} \cdot FS \cdot P_{RTITN}}{4\pi\rho\beta^3} M_0 \frac{(2\pi f)^2}{1+(f/f_c)^2} \frac{1}{\sqrt{1+(f/f_{\max})^m}} \frac{1}{R_C} \exp\left(-\frac{\pi f R}{Q(f)\beta}\right) \tag{2}$$

$$f_c = 4.9\times10^6 \beta \left(\Delta\sigma / M_0\right)^{\frac{1}{3}} \tag{3}$$

$$Q(f) = C_{Qc}\ f^{C_{Qp}} \tag{4}$$

$$\tau = \alpha_{tr}\ W / V_r \tag{5}$$

$$C_{Sa} = S_a\ /\ S \tag{6}$$

$$V_r = C_{Vr}\,\beta \tag{7}$$

where, $A(f)$ is the Fourier amplitude spectrum of ground motion acceleration from discrete fault element (cm/s); $R_{\theta\phi}$ is the radiation pattern; FS is the amplification due to the free surface (=2); P_{RTITN} is the reduction factor that accounts for the partitioning of energy into two horizontal components (=1); and m is the coefficient of the decay rate at high frequencies (=4.2). ρ is the density (g/cm^3); M_0 is the seismic moment of the fault element (N m); f_c is the corner frequency (Hz); β is shear velocity (km/s); $Q(f)$ is the Q-value; τ is rise time (s), which is the rapture time of fault element, W is the fault width (km); V_r is the rupture velocity (km/s); S_a is the area of asperity (km^2); and S is the area of fault (km^2)

CHARACTERISTICS OF GENERATED GROUND MOTIONS

The results of ground motion generation with MCS are shown in the following section. In order to obtain these results, 106,552 simulations were required to reproduce 200 ground motions.

Median and variation of maximum acceleration of generated ground motions

Figure 3 shows the coefficients for fitting the median to the attenuation relationship and the variations of generated ground motion accelerations. For crustal earthquakes, almost all sources are directly under the site and their distances are included in 6~8 km because of smaller magnitude. It can be seen that about 1.0 of the coefficient is enough for crustal earthquakes whose fault distance is relatively shorter to fit to the attenuation relationship. Most inter-plate earthquakes are Southern Kanto earthquakes whose fault distances are 40~60 km. Coefficients of about 1.5 are required for inter-plate earthquakes. The coefficients for intra-plate earthquakes are almost same as those of inter-plate earthquakes in cases of similar distance. However, the coefficients become larger as the distances increase, and coefficients of about 3~4 are required for fault distances exceeding 100 km.

The variations of stochastic parameters for seismic sources whose distances are 40~110 km are applied same values, which are listed in the 'others' row in Table 4. Smaller variations are given to crustal earthquakes and to subduction-zone earthquakes along the Japan Trench. It can be seen in Figure 3 that the variations of generated ground motion accelerations for crustal earthquakes reaches to 0.25~0.28 and there is scanty correlation between variations and fault distances. On the other hand, the variations of subduction-zone earthquakes, whose distances are 40~110 km, tend to become larger according to the distance. The variation of intra-plate earthquakes along the Japan Trench, whose distances are about 120 km, is about 0.23, which is lower than the target variation of 0.25.

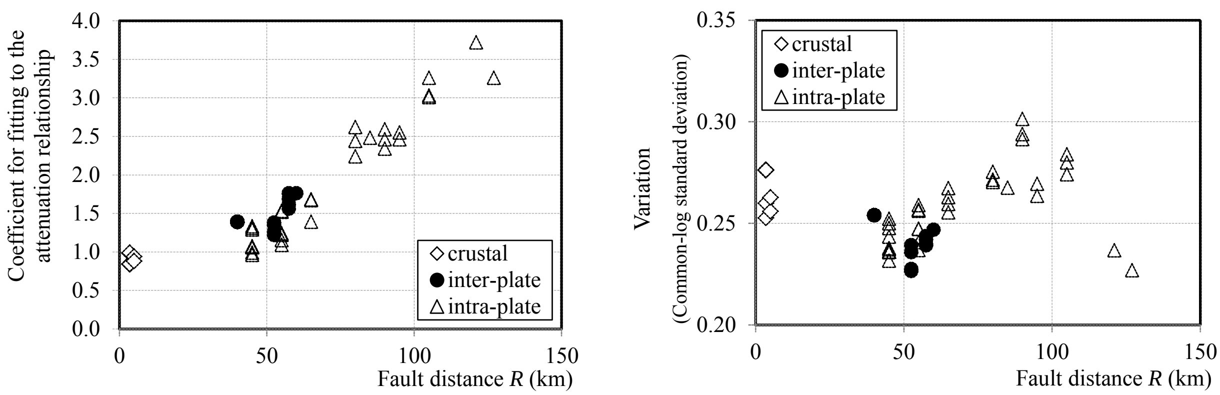

Figure 3. Coefficients for fitting to attenuation relationship and variations of generated ground motions.

A comparison between the accumulated frequency curve of the maximum acceleration for all generated ground motions and the hazard curve by attenuation relationship with 0.25 of variation can be seen in Figure 4. Ground motion generations were conducted for sources that yielded strong accelerations, so the curve by generated ground motions does not agree with the hazard curve by attenuation relationship for low accelerations. However, when it is focused on the target range from 700~1,100 cm/s^2, these two curves match each other. From this range, 200 ground motions are extracted as the reproduced ground motions.

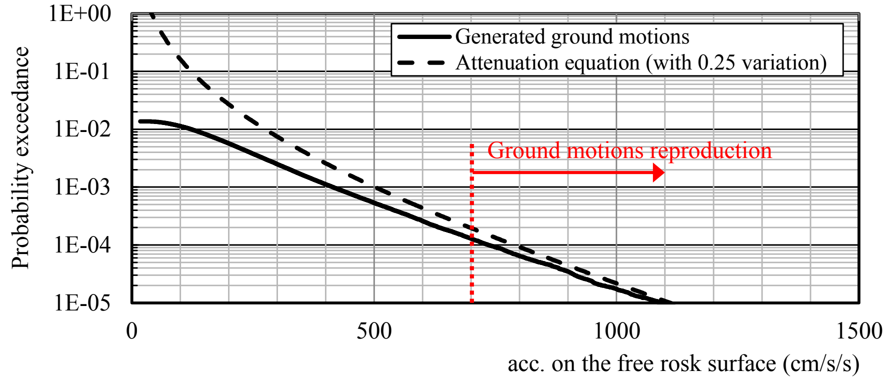

Figure 4. Comparison of hazard curves by generated ground motions and by attenuation relationship.

Characteristics of time histories and response spectra of reproduced ground motions

Figure 5 shows an example of time histories for reproduced ground motions. Waves are motion in the EW direction of fault-specified earthquakes in the Southern Kanto, fault-unspecified pacific plate earthquakes, and fault-unspecified crustal earthquakes. These ground motions are for the same hazard level, however, it can be seen that the arrival time of crustal earthquakes is shorter than those of subduction-zone earthquakes, and that durations of fault-specified earthquakes in the Southern Kanto and Pacific plate earthquakes are longer than for crustal earthquakes.

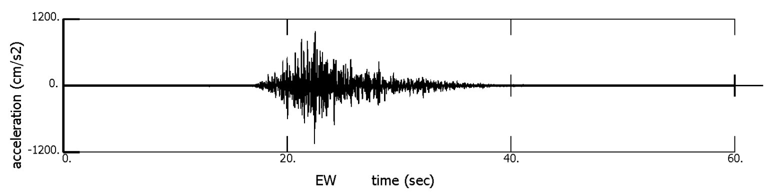

(1) Fault-specified earthquakes in the Southern Kanto

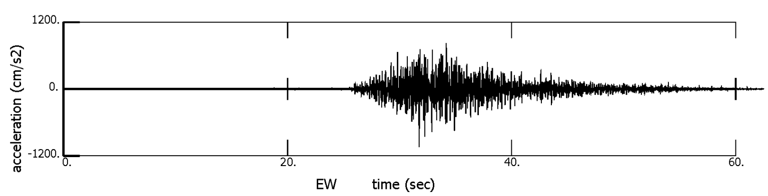

(2) Fault-unspecified pacific plate earthquakes

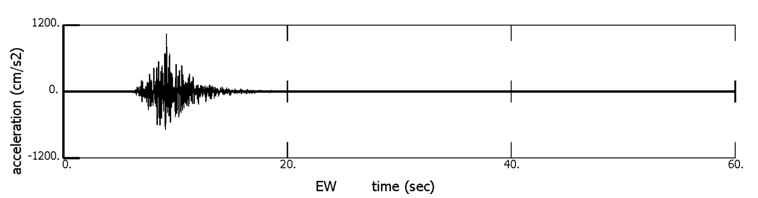

(3) Fault-unspecified crustal earthquakes

Figure 5. Example for time histories of reproduced ground motions (~1,000 cm/s^2).

Figure 6 shows the response spectra by reproduced ground motions of each source above, where the two curves are for the EW and NS directions. Fig. (1) shows the averaged spectra of 33 motions by fault-specified earthquakes in the Southern Kanto; Fig. (2) shows 7 motions by Pacific earthquakes, and Fig. (3) shows 6 motions by crustal earthquakes. A comparison of these spectra reveals that there is little difference between seismic sources, although the 0.05 sec of the spectra of the crustal earthquake is a little bit smaller than that of other sources.

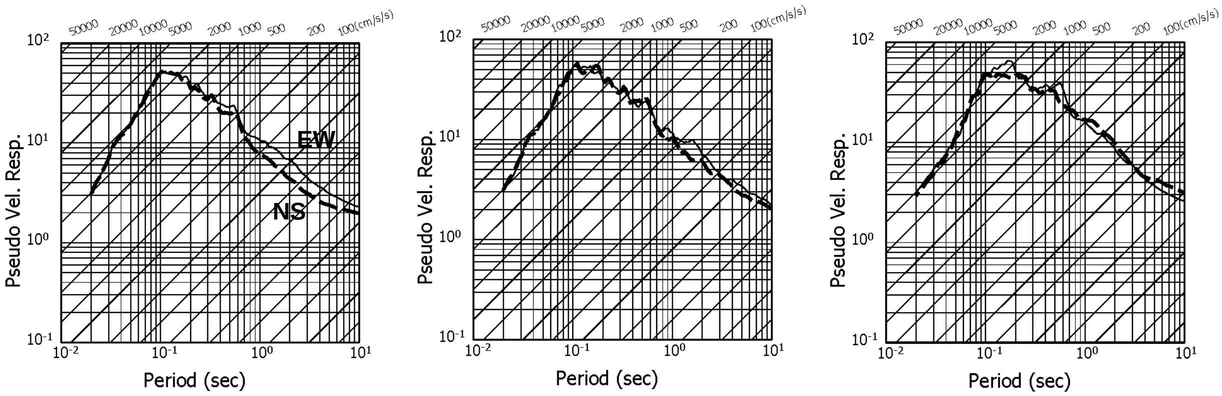

(1) Fault-specified/Southern Kanto (2) Pacific plate (3) Crustal

Figure 6. Example for response spectra of reproduced ground motions (~1,000 cm/s^2).

Seismic source characteristics of reproduced ground motions

Figure 7 shows the relationships between stochastic parameters deviations of seismic source characteristics and the maximum acceleration deviations of the reproduced 50 ground motions from 1,000 to 1,100 cm/s^2. The 'deviation' is the deviation of the value of reproduced (extracted) motion from the median of all generated motions for the same seismic source. It can be seen that acceleration deviations range from 1.5 to 3.0 and that these 50 motions have larger accelerations than the median acceleration generated from sources of equivalent magnitude and distance. It can be also seen that deviations of 1.0~3.0 for stress drops as well as positive deviations for high-cut filter frequencies and for Q-value coefficients are required for obtaining these acceleration deviations. On the other hand, there are little correlation between maximum accelerations and deviations for asperity area ratio or location of asperity. A similar tendency can be seen for other acceleration ranges, 700~1,000 cm/s^2.

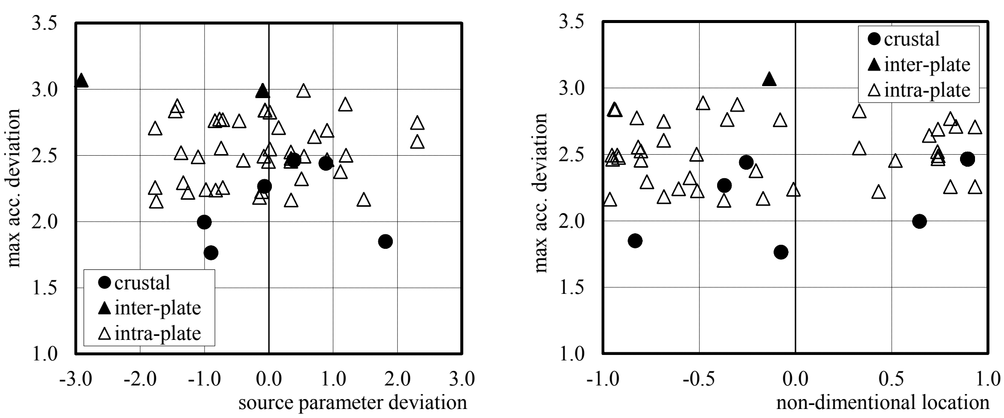

(1) asperity area ratio C_{Sa} (2) location of asperity aspX

Figure 7. Seismic source characteristics of reproduced ground motions.

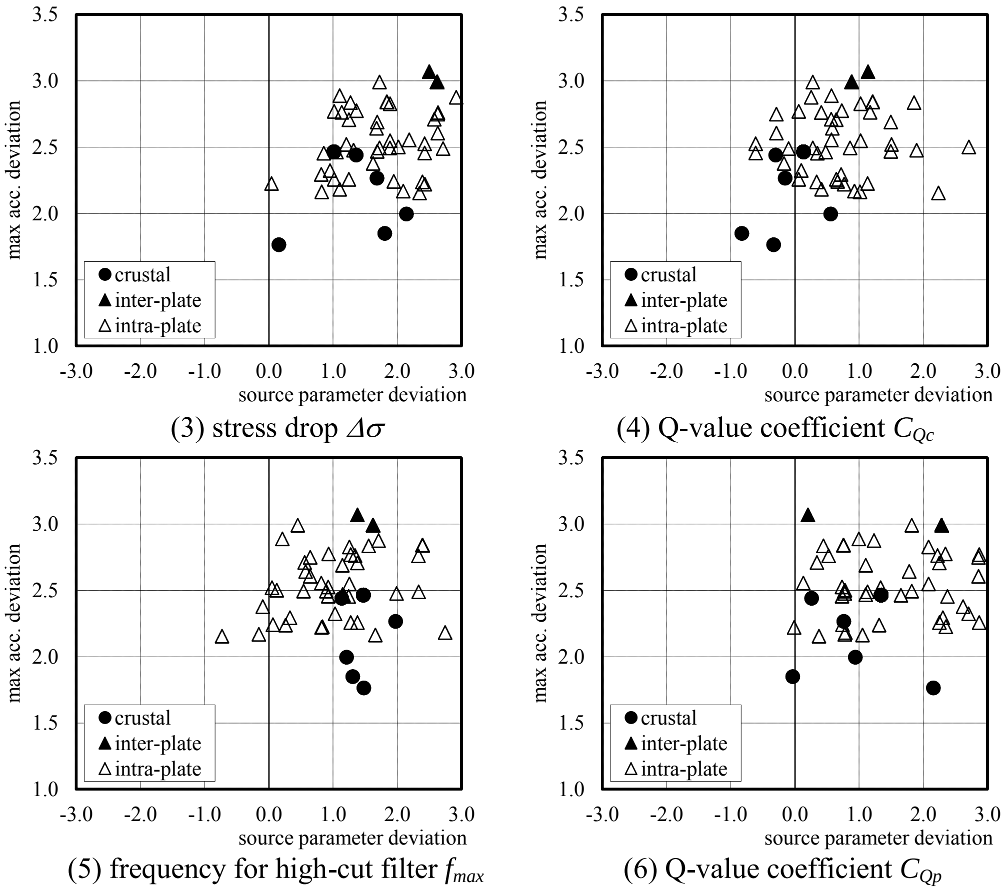

Figure 7. Seismic source characteristics of reproduced ground motions (continuation).

CONCLUSION

In this paper, the authors proposed a methodology based on MCS for reproducing a set of input ground motions to develop an advanced PRA scheme. A total of 200 ground motions were reproduced for a maximum acceleration range of 700 cm/s^2 to 1,100 cm/s^2, which corresponds to the acceleration level of design motion and to the annual exceedance probability of 10^{-5}, respectively.

Ground motions are generated by a stochastic Green's function method; in this way, they are intended to be consistent with the attenuation relationships used for seismic hazard evaluation. For this reason, the coefficients are multiplied to the generated motions, and stochastic parameters of seismic source characteristics are adjusted so that the variations of attenuation relationships are well reproduced.

These ground motions reproduced by the proposed method have individual characteristics depending on their seismic sources, whose characteristics are known in detail. A set of these ground motions, whose characteristics are known, will be available effectively for Probabilistic Risk Assessment (PRA) of the structure. As this method is still in progress, initial use has highlighted some issues and future refinements will focus on the following areas:

1) Ground motion generation was conducted to be consistent with one attenuation relationship, while there are many proposed relationships. The target relationship should be examined in more detail, which is essential for the seismic hazard analysis.
2) Stochastic parameters for seismic sources should be considered further. In recent years, the variation properties of seismic source characteristics have gradually emerged because of expansion of the seismography network. Still, there are many issues regarding seismic source uncertainty that should

be considered. In this context, only aleatory uncertainty of seismic source characteristics is considered, however, it is also important to consider epistemic uncertainty using logic Tree analysis.

3) The prediction accuracy of simulated ground motions by the stochastic Green's function method should be improved. The maximum acceleration of the generated ground motions is highly consistent with that of attenuation relationship when the fault distance of seismic sources is relatively short. On the other hand, it is not consistent when the fault distance of seismic sources is long.

REFERENCES

Architectural Institute of Japan (2004). "Ground vibration -phenomenon and theory- (in Japanese)"

Boore, D. M. (1983). "Stochastic Simulation of High-Frequency Ground Motions Based on Seismological Models of the Radiated Spectra", *Bulletin of Seismological Society of America*, 73(6) 1865-1894.

Dan, K. et al. (2001). "Short-period Source Spectra Inferred from Variable-Slip Rupture Models and Modeling of Earthquake Faults for Strong Motion Prediction by Semi-Empirical Method (in Japanese)", *J. Struct. Constr. Eng.*, AIJ, 545, 51-62.

Geller, R. J. (1976). "Scaling Relations for Earthquake Source Parameters and Magnitudes", *Bulletin of Seismological Society of America*, 66(5), 1501-1523.

Headquarters for Earthquake Research Promotion (2009). "Technical Report on National Seismic Hazard Maps for Japan (in Japanese)", Japan.

Itoi, T. et al. (2009). "Variability in Response Spectra for Crustal Earthquake using Stochastic Green's Function Approach (in Japanese)", *Journal of JAEE*, 9(1), 128-142.

Irikura, K. et al. (1997). "Revision of the empirical Green's function method by Irikura (1986) (in Japanese)", *Journal of SSJ*, 2, B25

Kamae, K. et al. (1991). "Prediction of Strong Ground Motion Based on Scaling Law of Earthquake (in Japanese)", *J. Struct. Constr. Eng.*, AIJ, 430, 1-9.

Kawase, H. and Matsuo, H. (2004). "Separation of Source, Path, and Site effects based on the Observed Data by K-NET, KiK-net, and JMA Strong Motion Network (in Japanese)", *Journal of JAEE*, 4(1), 33-52.

Mai, P. M. et al. (2005). "Hypocenter Locations in Finite-Source Rupture Models," *Bulletin of Seismological Society of America*, 95(3), 965-980.

Masuda, T. and Yokota, T. (2006). "Characteristics of asperities (in Japanese)", Proc. of *SSJ Annual Conference*, 124.

Satoh, T. et al. (1994a). "Statistical Special Characteristics for Engineering Bedrock Waves in which Local Site Effects of Surface Geology are Removed (in Japanese)", *J. Struct. Constr. Eng.*, AIJ, 462, 79-89.

Satoh, T. et al. (1994b). "Engineering Bedrock Waves Obtained through the Identification Analysis Based on Borehole Records and their Statistical Envelope Characteristics (in Japanese)", *J. Struct. Constr. Eng*, AIJ, 461, 19-28.

Satoh, T. et al. (2000). "High Frequency Fourier Spectra of Strong motions $-f_{max}$ and stress drop- (in Japanese)", *J. Struct. Constr. Eng.*, AIJ, 527, 79-87.

Satoh, T. (2004). "Short-period Spectral Level of Intra-plate and Inter-plate Earthquakes Occurring off Miyagi Prefecture (in Japanese)", *Journal of JAEE*, 1-4.

Sewell, R. T. et al. (2009). "Damage-Relevant PSHA", *Workshop Proceedings of Recent Findings and Developments in Probabilistic Seismic Hazards Analysis (PSHA) Methodologies and Application*, 509-542.

Si, H. and Midorikawa, S. (1999). "New Attenuation Relationships for Peak Ground Acceleration and Velocity Considering Effects of Fault Type and Site Condition (in Japanese)", *J. Struct. Constr. Eng.*, AIJ, 523, 63-70.

Tsurugi, M. et al. (2006). "Study on The Characteristics of Stress Drop for The Earthquakes Occurred in Kinki Region (in Japanese)", *Proc. of 12th JEES*, 378-381.